Supplementary Materials

Structure and Switchable dielectric properties of dabco complex with chromium chloride

A.Cizman[a*], D.Kowalska[b], M.Trzebiatowska[b], W.Medycki[c], M.Krupiński[d], P.Staniorowski[e], R.Poprawski[a]

[a]*Wrocław University of Science and Technology, Department of Experimental Physics, 27 Wybrzeże Wyspiańskiego, 50-370 Wrocław, Poland.*
[b]*Institute of Low Temperature and Structure Research, Polish Academy of Sciences, Okólna 2, 50-422 Wrocław, Poland.*
[c] *Institute of Molecular Physics, Polish Academy of Science, M. Smoluchowskiego 17, 60-179 Poznań, Poland.*
[d] *Institute of Nuclear Physics, Polish Academy of Sciences, Radzikowskiego 152, Krakow, Poland*
[e] *Institute of Experimental Physics, University of Wrocław, Pl. M. Borna 9, 50204 Wrocław, Poland*

† e-mail: agnieszka.cizman@pwr.edu.pl

CAPTIONS OF FIGURES

CAPTIONS OF TABLES

Structural information

Table S1. Octahedral distortion parameters Δd, d_G, Σ, and angle variance σ^2 of **DabcoCrCl**.

	Phase I	Phase II
T(K)	330	150
Ä*d*	0.0051	0.0053
d_G	0.0109	0.0096
Ó	18.28	17.71
ó^2	5.34	4.67

Δd – bond length distortion (Lufaso, 2004); σ^2 – octahedral angle variance (Fleet, 1976)

Table S2. The hydrogen-bond geometry (Å, º) of **DabcoCrCl** (phase I).

D—H···*A*	*D*—H	H···*A*	*D*···*A*	*D*—H···*A*
O1—H1*C*···Cl1^{i}	0.97	2.69	3.457 (4)	137
O1—H1*D*···Cl3^{ii}	0.97	2.17	3.115 (3)	165
O2—H2*C*···Cl3^{iii}	0.85	2.41	3.105 (3)	140
O3—H3···Cl3	0.86	2.25	3.079 (3)	161
N1—H1···Cl1	1.00 (1)	2.56 (2)	3.399 (3)	142 (2)
N1—H1···Cl2	1.00 (1)	2.45 (2)	3.228 (4)	134 (2)

Symmetry codes: ^{i} $x-1/2, y, -z+3/2$; ^{ii} $x-1/2, -y+1/2, -z+3/2$; ^{iii} $x-1/2, y, -z+5/2$.

All e.s.d.'s (except the e.s.d. in the dihedral angle between two l.s. planes) are estimated using the full covariance matrix. The cell e.s.d.'s are taken into account individually in the estimation of e.s.d.'s in distances, angles and torsion angles; correlations between e.s.d.'s in cell parameters are only used when they are defined by crystal symmetry. An approximate (isotropic) treatment of cell e.s.d.'s is used for estimating e.s.d.'s involving l.s. planes.

Table S3. The hydrogen-bond geometry (Å, º) of **DabcoCrCl** (phase II).

D—H···*A*	*D*—H	H···*A*	*D*···*A*	*D*—H···*A*
O1—H1*C*···Cl4	0.80	2.26	3.043 (3)	165
O1—H2*D*···Cl5^{i}	0.92	2.17	3.060 (3)	162
O2—H2*C*···Cl5^{ii}	0.85	2.42	3.105 (3)	138
O2—H2*D*···Cl4^{iii}	0.79	2.32	3.079 (3)	164
O3—H3*C*···Cl5	0.89	2.33	3.137 (4)	151
O3—H3*D*···Cl4^{iv}	0.88	2.20	3.068 (3)	167
N1—H1···Cl1	0.98	2.55	3.351 (4)	139
N1—H1···Cl2	0.98	2.46	3.211 (4)	133
N2—H2···Cl1^{v}	0.98	2.54	3.353 (4)	140
N2—H2···Cl3^{v}	0.98	2.56	3.296 (4)	132

Symmetry codes: ^{i} $-x+1, y-1/2, -z+1/2$; ^{ii} $x+1, y, z$; ^{iii} $-x+2, y+1/2, -z+1/2$; : ^{iv} $-x+1, y+1/2, -z+1/2$; ^{v} $-x+1/2, -y+1, z+1/2$.

All e.s.d.'s (except the e.s.d. in the dihedral angle between two l.s. planes) are estimated using the full covariance matrix. The cell e.s.d.'s are taken into account individually in the estimation of e.s.d.'s in distances, angles and torsion angles; correlations between e.s.d.'s in cell parameters are only used when they are defined by crystal symmetry. An approximate

(isotropic) treatment of cell e.s.d.'s is used for estimating e.s.d.'s involving l.s. planes.

IR and Raman information

Table S4: The wavenumbers (cm^{-1}) of the observed Raman and infrared bands of **DabcoCrCl** at room temperature.

Wavenumbers (cm^{-1})		**Assignment**
IR	**Raman**	
3242vs		νOH νNH
3147sh		νOH νNH
3064vs	3063w	$\nu_{as}CH_2$
3023sh	3022s	$\nu_{as}CH_2$ ν_sCH_2
	2997s	ν_sCH_2
	2974vs	ν_sCH_2
	2947vw	ν_sCH_2
	2913m	ν_sCH_2
2817w	2775vw	combination
2631vw		combination
1652sh		δNH
1617s		δOH
1522w		δNH δOH
1473m	1462w	δCH_2
1462m		δCH_2
1435w		δCH_2
1407s		τCH_2
1388m	1395vw	τCH_2
	1363vw	ωCH_2
1320w	1319vw	ωCH_2
	1265w	ρCH_2
1200vw		ρCH_2
	1158vw	ν_{as}CNC ν_{as}CCN ρCH_2
1054s	1052w	ν_{as}CNC ν_{as}CCN
	976w	ν_sCNC ν_sCCN
885w	891w	ρOH
846m	848vw	ρOH
802w	804m	ρOH
599vw	601w	ν_sCNC ν_sCCN
	555vw	δCNC δCCN
	439vw	νCrO δCNC δCCN T'O
	405w	νCrO δCNC δCCN T'O
	314m	νCrCl T'dabco T'O

	292m	vCrCl T'dabco T'O
	258w	vCrCl T'dabco
	232w	T'dabco T'Cl
	175w	Ldabco T'Cl
	127w	Ldabco T'Cl

Key: s-very strong, s-strong, m-medium, w-weak, vw-very weak, sh-shoulder; ν_s–symmetric stretching, ν_{as}-asymmetric stretching, δ-in-plane bending (scissoring), ρ-rocking, ω-wagging, τ-twisting (torsion), T–translation, L–libration.

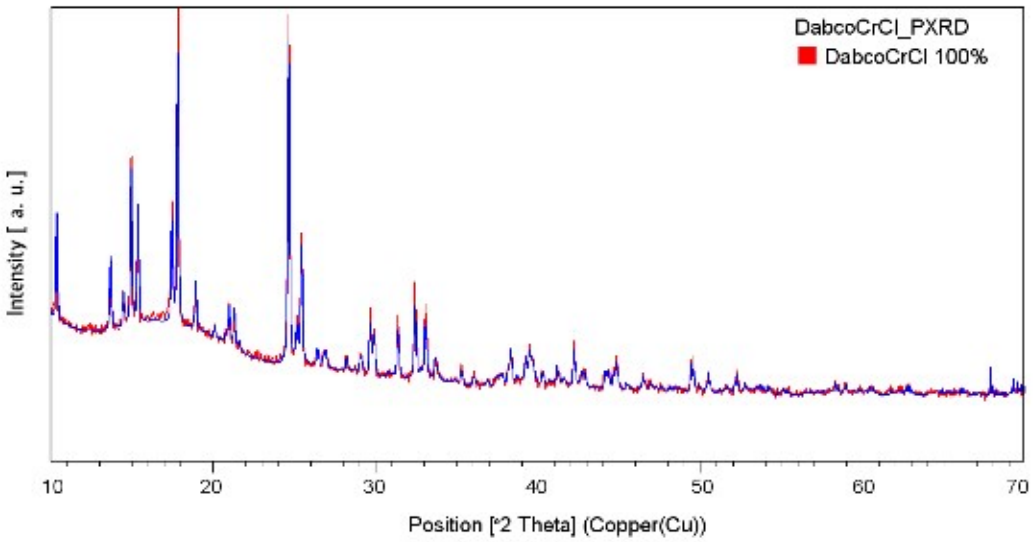

Figure S1 Powder XRD pattern for **DabcoCrCl** together with the calculated one based on the *Pnma* single crystal structure at room temperature.

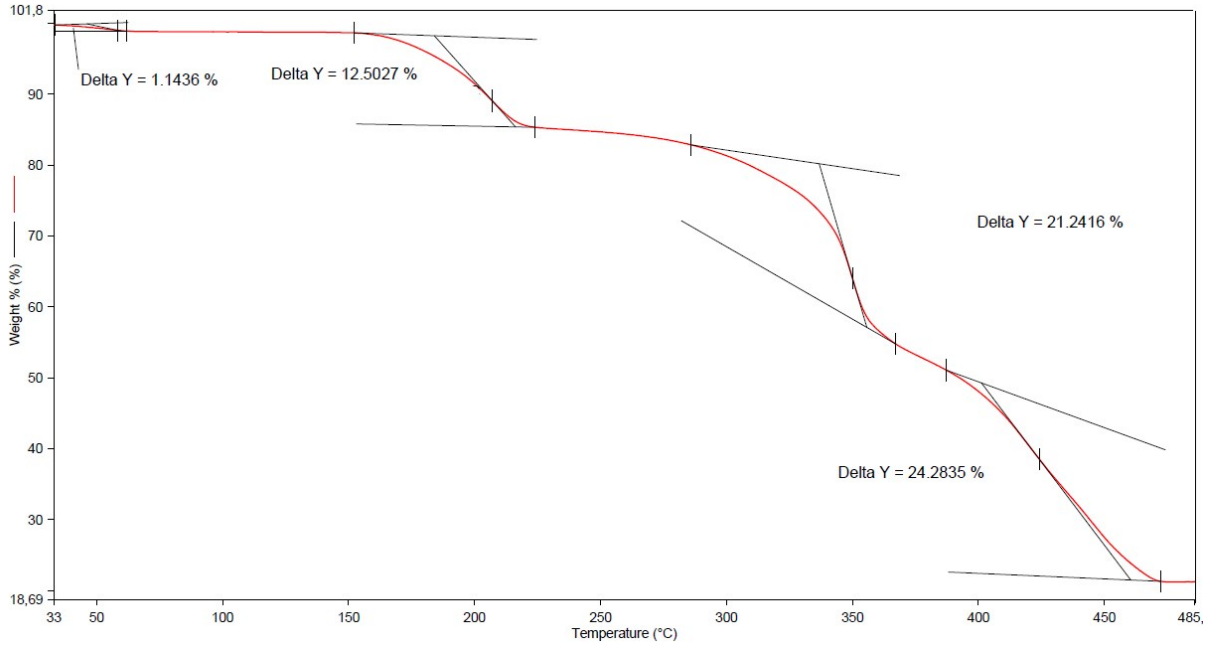

Figure S2. Simultaneous thermogravimetric (TG) scan of **DabcoCrCl** (ramp rate: 5 K min^{-1}).

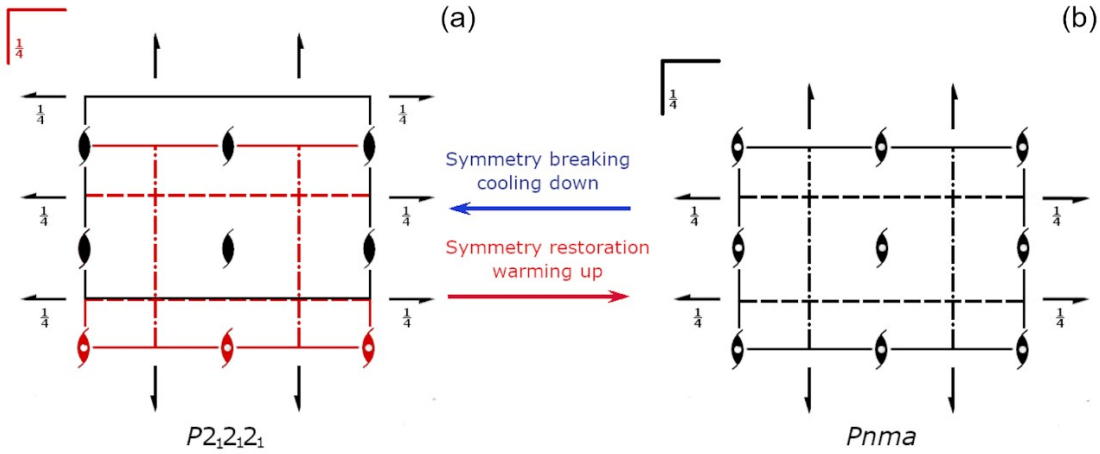

Figure S3. The symmetry element comparison of Phases I (b) and II (a). The symmetry elements that disappear in Phase II are shown in red color. The relationship between unit cell axes is as follows: $a_{II} = c_I$, $b_{II} = a_I$, $c_{II} = b_I$.

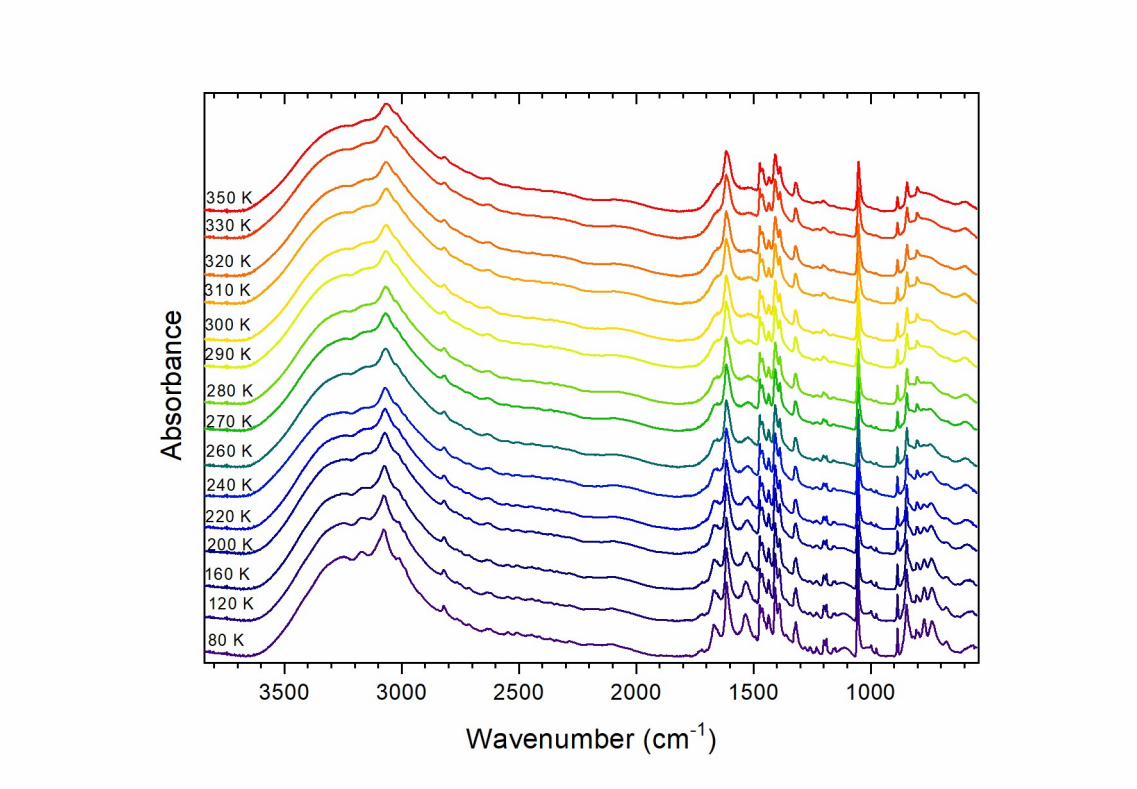

Figure S4. The temperature-dependent IR spectra of **DabcoCrCl**.

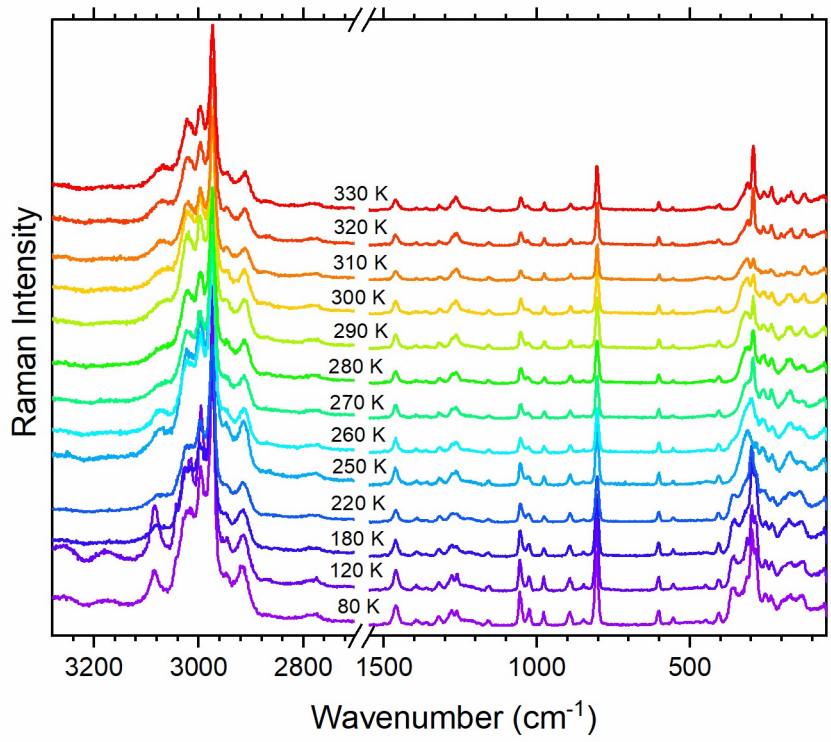

Figure S5. The temperature-dependent Raman spectra of **DabcoCrCl**.

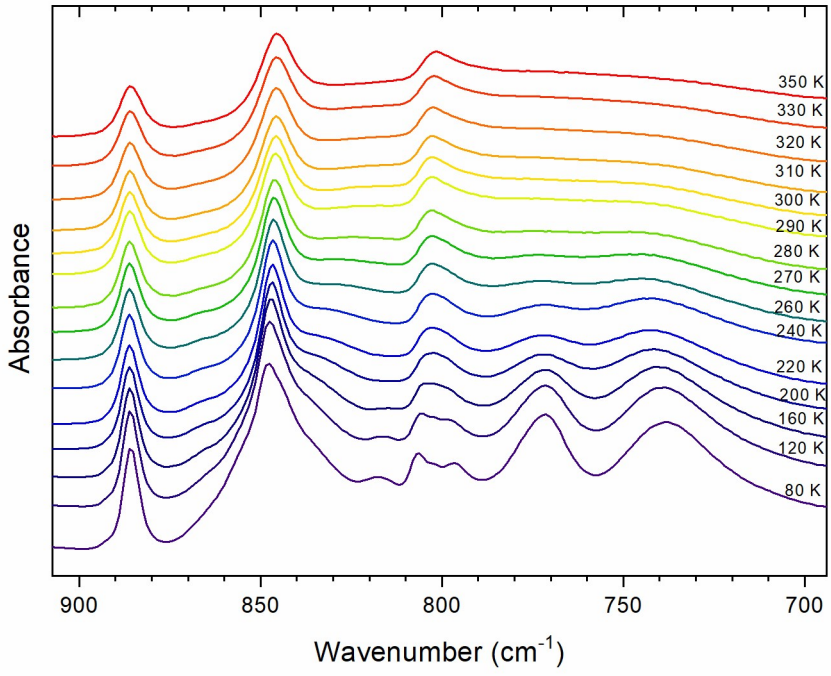

Figure S6. The temperature-dependent IR spectra of **DabcoCrCl** within the range of deformation vibrations of water molecules.

The M(T) curve measured at a small external magnetic field of 100 Oe is shown in Figure S5b. The same data are also depicted in Figure S5a as a function of inverse temperature M(1/T). The shape of the dependencies is typical for paramagnetic materials and agrees very well with Curie's law, which suggests that **DabcoCrCl** is a paramagnetic in the whole studied temperature range. The M(H) measurement at 300 K is shown in Figure S6. It also presents classic behaviour for paramagnetic materials – a linear relationship being an approximation of the Brillouin function at high temperature. The determined mass magnetic susceptibility at 300 K amounts to χ_{mass} = 1.7*10^{-5} emu/g*Oe.

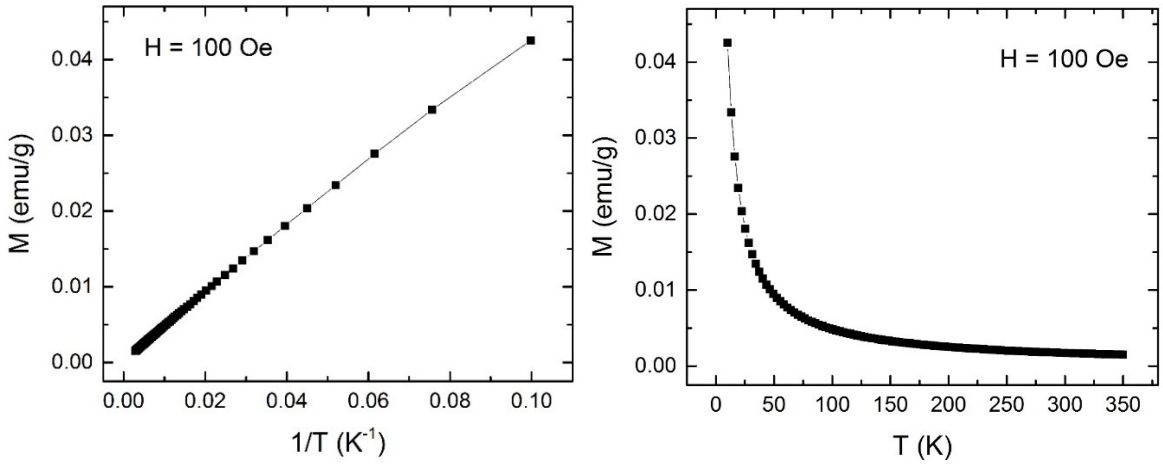

Figure S7. (a) The magnetic moment as a function of temperature at external magnetic field at 300 K. (b) The same data depicted as a function of inverse temperature.

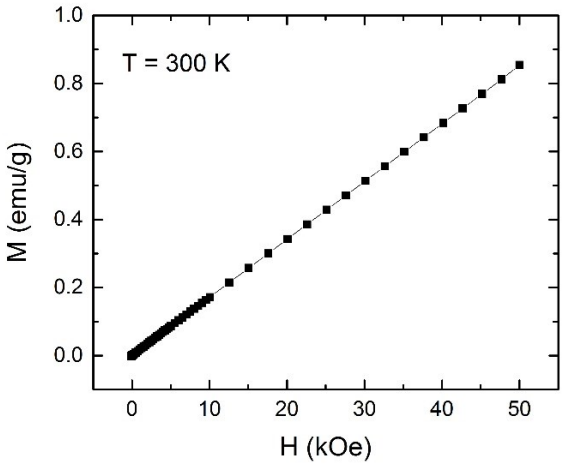

Figure S8. The M(H) curve measured at 300 K.